



# Calibration of Aerogel Tiles for the HELIX-RICH Detector

P. Allison<sup>a</sup>, J. J. Beatty<sup>a</sup>, L. Beaufore<sup>b</sup>, Y. Chen<sup>c</sup>, S. Coutu<sup>c</sup>, E. Ellingwood<sup>f</sup>, N. Green<sup>e</sup>, \*D. Hanna<sup>f</sup>, H. B. Jeon<sup>b</sup>, B. Kunkler<sup>d</sup>, M. Lang<sup>d</sup>, R. Mbarek<sup>b</sup>, K. McBride<sup>a</sup>, I. Mognet<sup>c</sup>, J. Musser<sup>d</sup>, S. Nutter<sup>g</sup>, \*\*S. O'Brien<sup>f</sup>, N. Park<sup>h</sup>, T. Rosin<sup>f</sup>, Z. Siegel<sup>b</sup>, M. Tabata<sup>i</sup>, G. Tarlé<sup>e</sup>, G. Visser<sup>d</sup>, S. P. Wakely<sup>b</sup>, M. Yu<sup>c</sup>

\*hanna@physics.mcgill.ca \*\*stephan.obrien@mcgill.ca



HELIX (High Energy Light Isotope eXperiment) is a balloon-borne instrument designed to measure the chemical and isotopic abundances of light cosmic-ray nuclei. In particular, HELIX is optimized to measure Be-10 and Be-9 in the range 0.2 GeV/n to beyond 3 GeV/n. To achieve this, HELIX utilizes a 1 Tesla superconducting magnet with a high-resolution gas drift-tracking system, time-of-flight (ToF) detector, and a ring-imaging Cherenkov (RICH) detector. The RICH detector consists of aerogel tile radiators (refractive index  $\sim 1.15$ ) with a silicon photomultiplier detector plane. To adequately discriminate between Be-10 and Be-9 isotopes, the refractive index of the aerogel tiles must be known to a precision of 0.01%. In this contribution, detailed mapping of the refractive index across the aerogel tiles is presented and the methodology used to obtain these measurements is discussed.

## HELIX

High Energy Light Isotope eXperiment (HELIX, [1]) is a balloon-borne experiment designed to measure isotopic and chemical abundances of light cosmic-ray nuclei.

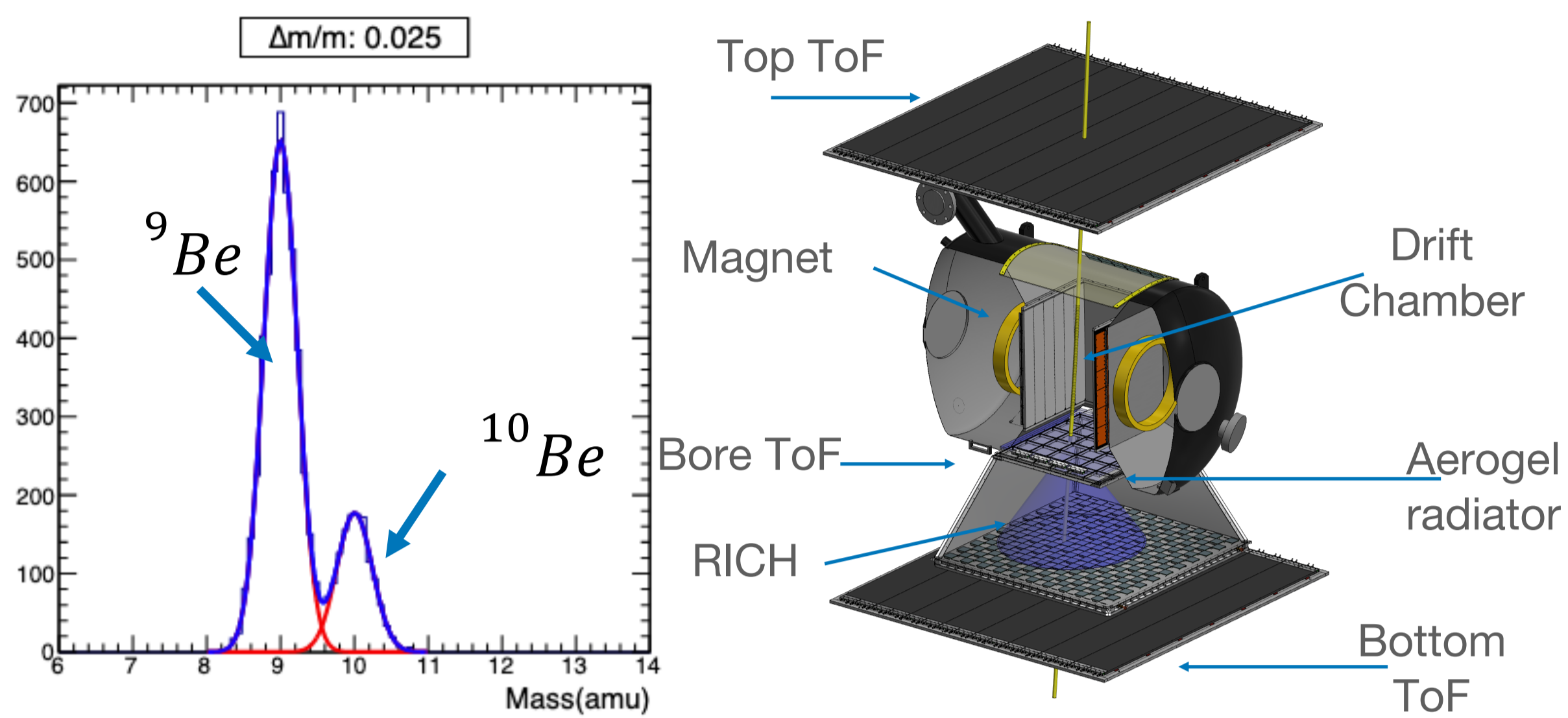


Fig 1. (Left) Expected  ${}^{10}\text{Be}$  and  ${}^9\text{Be}$  mass resolution. (Right) The HELIX experiment.

HELIX is optimised to measure the Be-10 to Be-9 ratio in the 0.2 to > 3. GeV/n range. HELIX utilises a 1 Tesla magnet and high-resolution gas drift-tracking system to measure particle rigidity. ToF counters and a RICH detector are used to measure particle velocities.

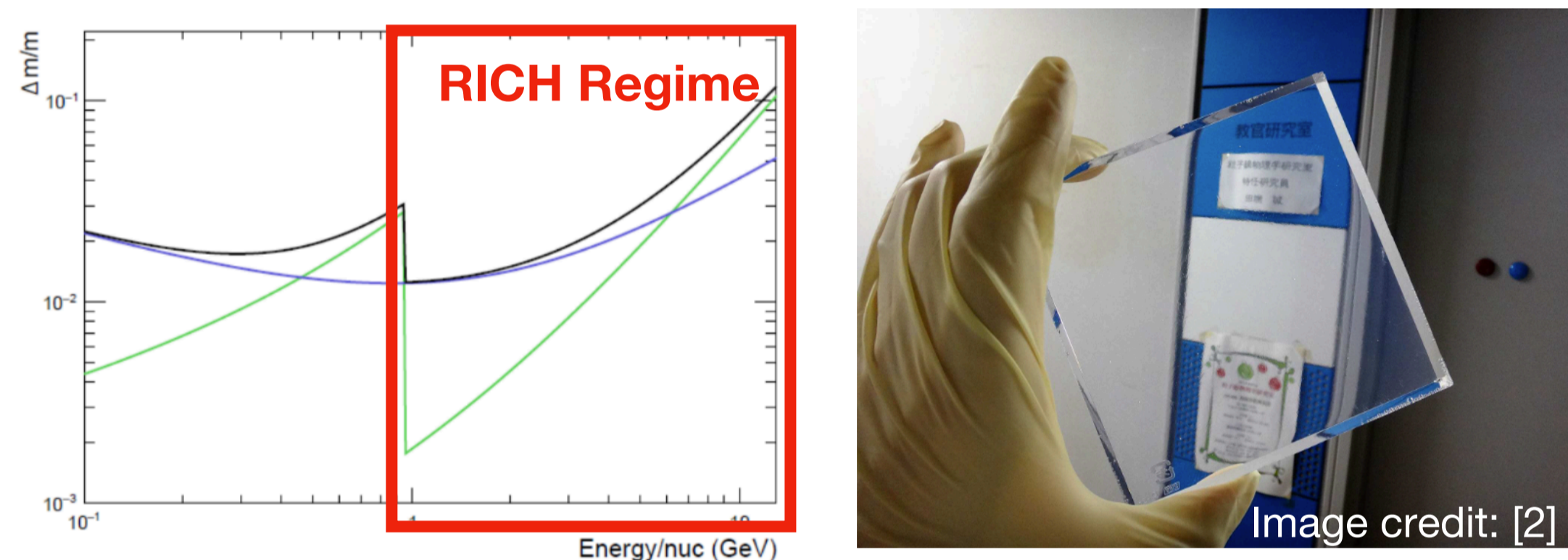


Fig 2. (Left) Predicted mass resolution of the HELIX-ToF and HELIX-RICH detectors. (Right) Image of a HELIX aerogel tile.

The HELIX RICH [3] consists of an aerogel radiator plane and a SiPM detector plane. The radiator plane is made up of 36 (6x6) high-refractive index ( $n \sim 1.15$ ) aerogel tiles (10cm x 10cm x 1cm) [2]. The RICH is designed to measure velocities of particles with E greater than 1 GeV/nucleon.

## Measuring The Refractive Index Using Relativistic Electrons

Precise measurements of the refractive index were made by measuring the Cherenkov ring produced by a beam of 35 MeV electrons from a linear accelerator at the National Research Council of Canada in Ottawa.

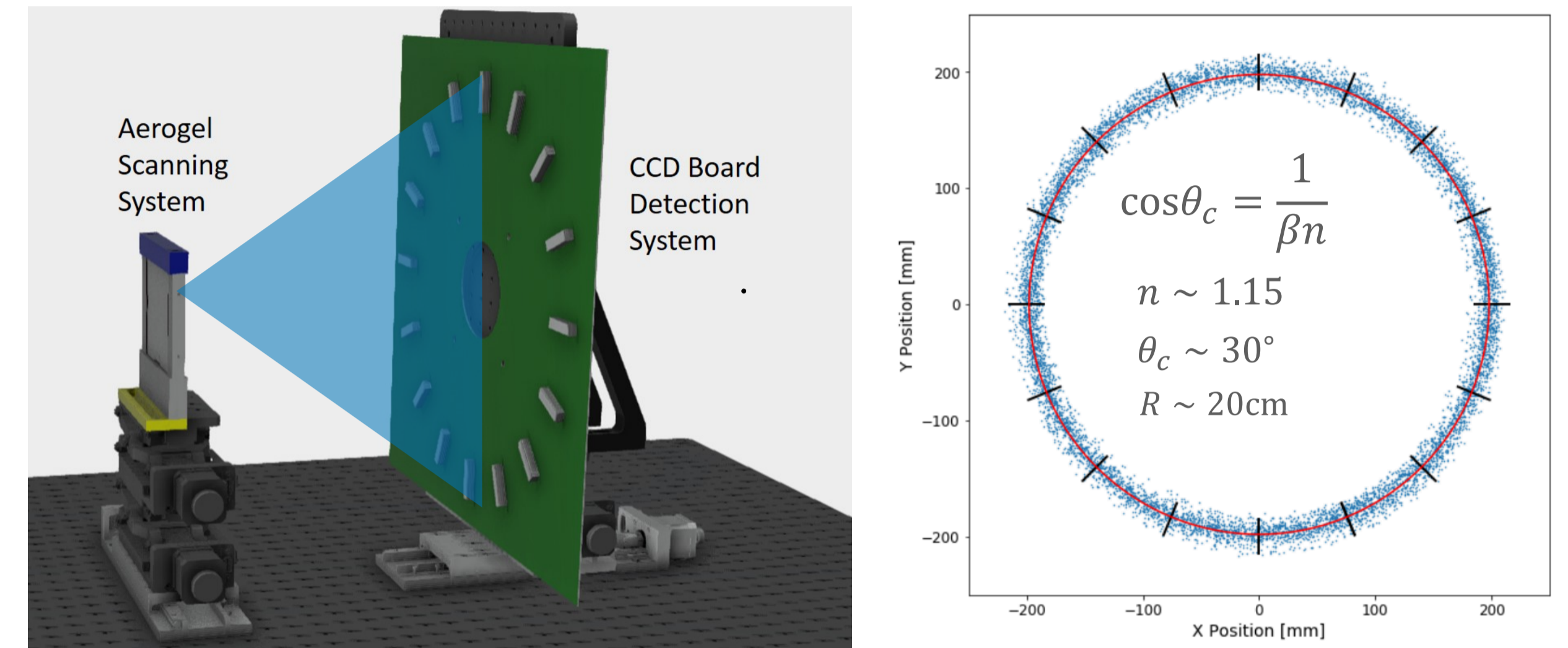


Fig 3. (Left) CAD image of CCD-detector board and aerogel scanning system. (Right) Simulated Cherenkov ring with CCD positions overlaid.

The Cherenkov ring is sampled using a CCD-detector board consisting of 16 one-dimensional CCDs (Toshiba TCD1304DG, 3694 pixels, each pixel  $8 \mu\text{m} \times 200 \mu\text{m}$ ) arranged in a circle of radius 20 cm at azimuthal increments of 22.5 degrees. The aerogel tile is mounted in a scanning frame, positioned by stepper motors, allowing for a 5mm-grid X-Y scan across the tile face. The CCD-detector board is mounted on an X-Y-Z stepper motor system, allowing for accurate positioning of the CCD-detector board with respect to the Cherenkov ring.

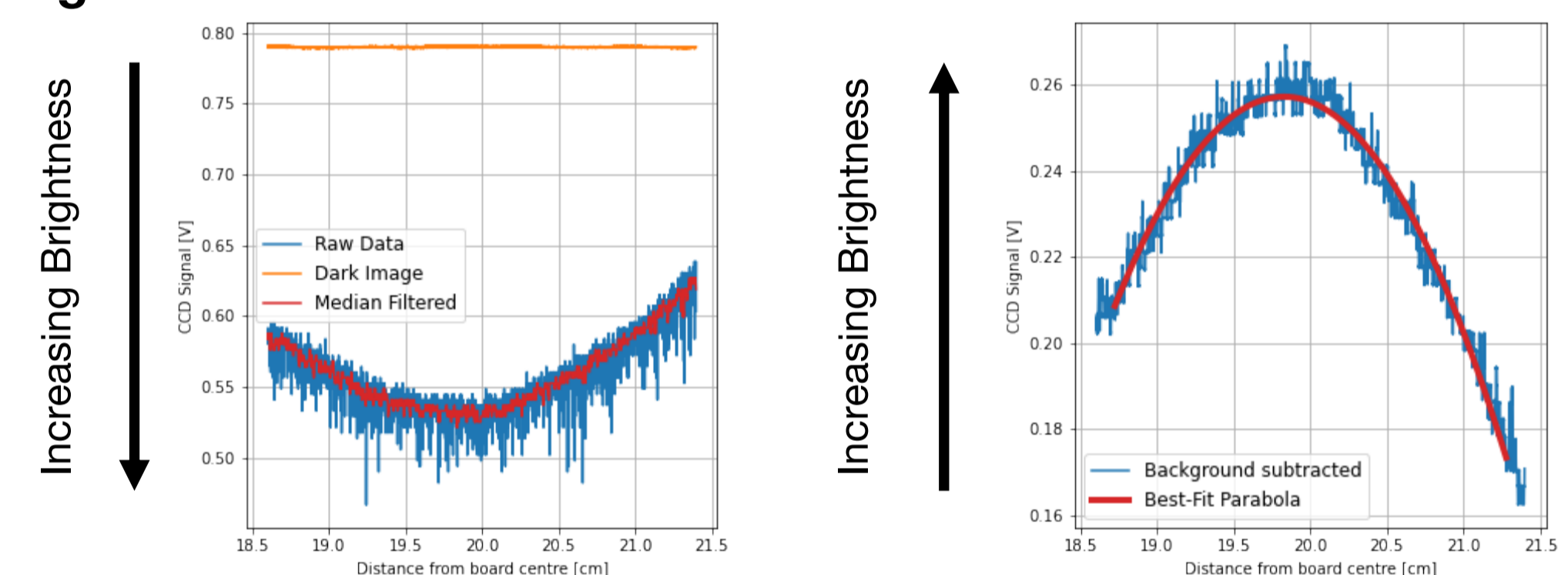


Fig 4. (Left) Example CCD trace. (Right) Background adjusted CCD trace with a median filter applied, and the best-fit parabola.

The CCD data are digitised using an Acqiris DC270 8 bit FADC. For each scan point, 100 "images", each corresponding to a beam pulse of  $\sim 10$  billion electrons, are obtained. Dark (beam-off) images are recorded prior to data taking to account for any background light sources. The background-subtracted image is well-described by a parabola, with the peak corresponding to the peak of the Cherenkov ring. The broadness of this distribution is due to divergence of the electron beam.

## Refractive Index Maps

The positions of the maxima of the fits to the CCD data are fit to a circle with centre and radius as free parameters. The refractive index ( $n$ ) is related to the measured ring radius ( $r$ ) by:

$$\tan\theta_c = n_0\beta \left( \frac{r - z_e \tan\theta_c}{\sqrt{(r - z_e \tan\theta_c)^2 + d^2}} \right), n = \frac{1}{\cos\theta_c\beta},$$

where  $z_e$  is taken to be the half-thickness of the aerogel,  $d$  is the expansion length of the Cherenkov cone and  $n_0$  is the refractive index of air. Thickness variations of the aerogel, measured using a coordinate measuring machine (CMM) at TRIUMF, are corrected for when calculating the refractive index. The setup can accurately measure a refractive index in the 1.150 - 1.165 range, with a statistical uncertainty of  $\Delta n/n \sim O(10^{-4})$ . Remote repositioning of the CCD-detector board allows for complete coverage of the expected refractive index range.

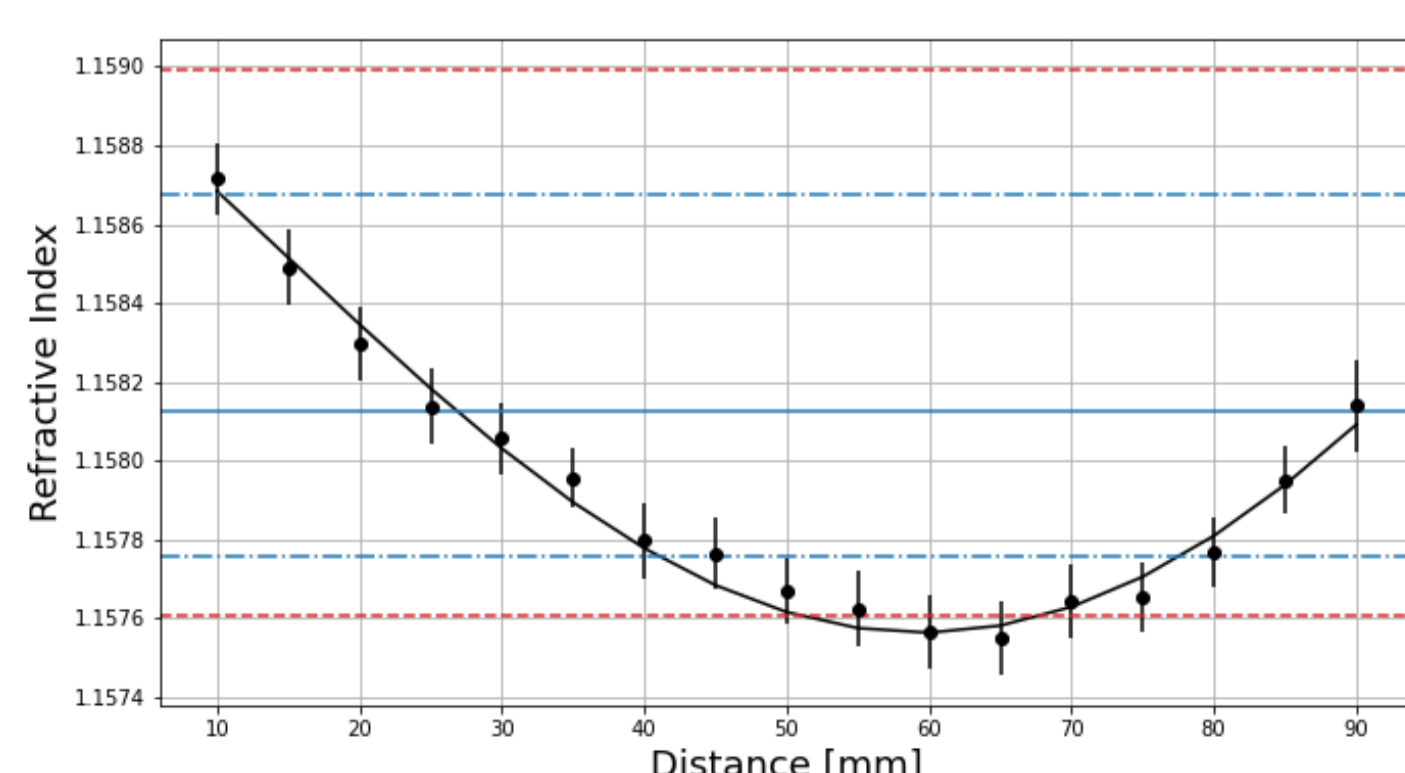


Fig 6 A slice across the refractive index map shown in Fig 5. The smooth curve is given by a two-dimensional parabola fit to the entire map.

The refractive index varies smoothly across the tile, with the variations well-fit by a 2D-parabola. A refractive index map is shown in Fig. 5 (left). The indices are histogrammed on the right. The median index is shown as a solid blue line and the 68% and 90% containment limits are shown as blue "dot-dashed" and red "dashed" lines respectively.

A slice across the same tile is shown in Fig. 6, along with the results of the 2D parabolic fit made to data from the whole tile.

Systematic effects, such as the effects of the varying aerogel thickness, multiple scatter of electrons and beam divergence, are currently being studied. Additional methods of calibration, such as a laser deflection method, are also being investigated [4]. Refractive index maps, along with precise thickness maps of the aerogel tiles, are being produced for the analysis of HELIX data.

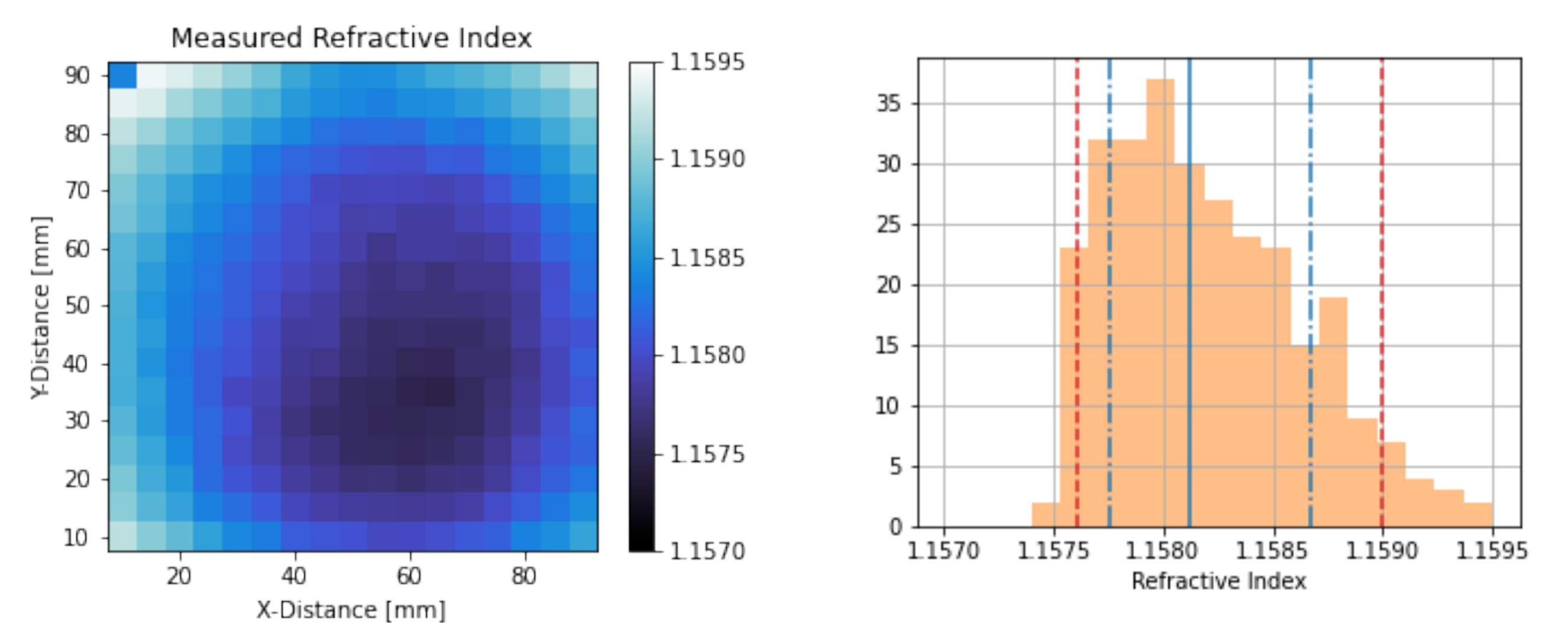


Fig 5 (Left) Map of measured refractive indices for a typical tile. (Right) Histogram of refractive indices from the same tile.